Evaluation of Neopentane–Deuterium Exchange on Pt/Al₂O₃ as a Probe for Physical Phenomena

GÜNSELI SAĞUN AND WILLIAM R. ERNST[1]

School of Chemical Engineering, Georgia Institute of Technology, Atlanta, Georgia 30332

The deuterium exchange of neopentane over Pt/Al₂O₃ was investigated in a batch recirculation reactor and found to exhibit many characteristics previously found for this reaction over Pd/SiO₂–Al₂O₃. All of the data could be correlated in terms of two parameters—k, the surface rate constant and β, the desorption parameter. The parameter β was less dependent upon k for the Pt catalyst than for Pd catalysts. Specific activity was not influenced by Pt dispersion; whereas selectivity was mildly sensitive to Pt dispersion.

I. INTRODUCTION

There is a need for well defined reactions that can be used as probes to study physical phenomena within commercial catalysts and catalytic reactors. Examples of such phenomena are intraparticle diffusion effects in porous catalysts (Dwyer *et al.* (*6, 7*); Ernst and Wei (*9*)), dispersion effects in laboratory reactors (Zahner (*21*)), and effects of active ingredient profiles in nonuniformly active catalysts (Ernst and Daugherty (*8*)).

In order for a reaction to be suitable as a probe for physical phenomena, it must have some property, such as activity or selectivity, or both, which is sensitive to the physical phenomena of the catalyst (or reactor) but insensitive to certain chemical properties—for example, state of metal dispersion in supported metal catalysts. It is also highly desirable that the reaction kinetics be well understood, both in the presence and absence of the physical phenomena being studied and that the experimental kinetic data be analyzable by relatively simple mathematical treatment.

The exchange of certain hydrocarbons with deuterium on supported metals have properties that make them good candidates

as probe reactions. The exchange of neopentane with deuterium is particularly ideal based on studies of the reaction on evaporated Pd films (Kemball (*10*); Mikovsky and Wei (*13*)). These observed desirable characteristics are

1. The reactions can be made pseudo-first order in neopentane in batch experiments employing a large excess of deuterium.

2. The surface mechanism appears to involve a single step exchange of H and D atoms.

3. Heat of reduction is negligible.

4. All of the hydrogen atoms in neopentane are equivalent.

5. Kinetic isotope effects are negligible.

6. The reaction yields 12 deuterated products. (This is an important feature especially for comparing the fit of different theoretical models.)

7. The reaction system can be easily analyzed using a mathematical technique developed by Wei and Prater (*18*).

Dwyer *et al.* (*6*) investigated the influence of intraparticle diffusion limitations on the neopentane–deuterium exchange over beds of Pd/SiO₂–Al₂O₃ catalyst beads. Kemball (*10*) previously showed on evaporated Pd films that this reaction, in the absence of diffusional effects, could be explained by a single-step surface exchange mechanism and produced a "binomial"

---

[1] To whom all correspondence should be addressed.

95

product distribution. If similar conditions existed on supported Pd catalysts, Dwyer would have been able to show that deviation of the product distribution from binomial character could be attributed to intraparticle diffusional resistances. However, Dwyer's work at higher temperatures was influenced by a desorption effect which was not important in Kemball's work over Pd films. Dwyer developed a theory to describe the surface reaction as a single-step surface exchange modified by desorption (or β) effects—where β is the ratio of characteristic time for desorption of·adsorbed species from the surface to the characteristic time for surface reaction. Dwyer successfully correlated all of his experimental kinetic data with a two-parameter model with ϕ, the Thiele modulus, characterizing intraparticle mass transfer influences and β characterizing desorption influences. Ernst and Wei (9) studied the same reaction over well-characterized single spherical catalyst beads in order to eliminate averaging effects that might have occurred in Dwyer's work due to the use of a bed of beads.

Neither Dwyer nor Ernst was able to avoid β effects over wide ranges of operating conditions. In both studies, reaction temperature and catalyst particle size were the primary variables used to adjust ϕ and β; however, temperature varied both ϕ and β. Varying particle size by cleaving or crushing produced the desired effect of lowering ϕ; however, the intrinsic catalyst activity, also decreased as particle size was reduced—probably because of contamination. The parameter β was found to vary linearly with intrinsic activity in both studies at low activity levels.

Dwyer et al. (7) investigated the effect of catalyst pretreatment on the catalyst selectivity. They showed that oxygen pretreatment greatly reduced the β parameter with respect to intrinsic activity and changed the observed reaction from apparent multistep to single step kinetics.

Thus, there is justification for pursuing research to evaluate other reaction–cata-

lyst systems as possible probes solely for mass transfer effects. The exchange of hydrocarbons over supported Pt is a good candidate primarily because of the importance of Pt as an industrial catalyst and the relative ease of recovering the activity of Pt after it has been deactivated by carbon or by exposure to adsorbing gases. Techniques for producing a wide variety of radial Pt concentration profiles within porous spherical catalyst beads have been recently developed (Shyr and Ernst (16)). Thus, supported Pt catalysts are a likely choice of systems when one is interested in studying the influence of radial concentration profiles of active ingredient on reaction activity or selectivity. The possibility also exists that the exchange reaction over Pt will exhibit a binomial product distribution in the absence of diffusional effects but that β effects will be less important than they are on Pd.

The primary objective of the present work was to determine the suitability of neopentane–deuterium exchange system as a possible probe reaction for studying physical phenomena in catalysts. Prior works on the neopentane–deuterium exchange reaction on Pt have been performed but were not reported in the open literature (Yurchak (20)).

The present work is aimed at studying some of the kinetic aspects of the reaction system. The first objective was to study the reaction kinetics over a wide range of operating conditions on supported Pt catalysts which are free of intraparticle and interparticle transport limitations and in a reactor which is free of dispersion effects. Such a study would reveal whether the reaction can be described in terms of a simple model such as one based on a single-step surface exchange mechanism, pseudo-first order in neopentane but with negligible isotope effects. The second objective was to attempt to explain any kinetic data which deviated from simple single-step behavior in terms of Dwyer's model of single-step exchange influenced by desorption effects. Once an un-

derstanding of the kinetics was established, the final objective was to determine the effect of Pt dispersion on kinetics and selectivity of the reaction.

II. THEORY

The vector equation which Dwyer developed to correlate reaction data for neopentane–deuterium exchange on supported Pd (6) in the absence of mass transport limitations is

$$\frac{d}{dt}\mathbf{a} = -k\mathbf{B}\left[I + \frac{\beta}{n}\mathbf{B}\right]^{-1}\mathbf{a} \quad (1)$$

where

a_i = mole fraction of $C_mH_{n-i}D_i$ in the hydride mixture (for t-butyl fragments of neopentane $m = 4$ and $n = 9$).

k = rate constant for exchange.

$\mathbf{B}$ = stoichiometric matrix which (for the case of negligible reverse reaction) has elements

$B(i,i) = (n - i)$ for $i = 0$ to n,

$B(i,i - 1) = -(n - i + 1)$ for $i = -1$ to n,

with all other elements equaling zero.

β = desorption parameter.

By applying the method of Wei and Prater (18) the solution to Eq. (1) can be shown, in terms of characteristic species, to be:

$$\mathbf{b} = \mathbf{b}^0 \exp\{-[k\Lambda't]\} \quad (2)$$

or, in terms of real species,

$$\mathbf{a} = \mathbf{X}\mathbf{b}$$

where

Λ' = eigenvalue matrix of $\mathbf{B}$ which has elements

$$\lambda_i' = \frac{i}{1 + \dfrac{i\beta}{12}} \quad (3)$$

$\mathbf{X}$ = eigenvector matrix of B. For example—for methane,

$$\mathbf{X} = \begin{bmatrix} 0 & 0 & 0 & 0 & 1 \\ 0 & 0 & 0 & 1 & -4 \\ 0 & 0 & 1 & -3 & 6 \\ 0 & 1 & -2 & 3 & -4 \\ 1 & -1 & 1 & -1 & 1 \end{bmatrix}$$

Equation (2) in elemental form is:

$$b_i = b_i^0 \exp[-k\lambda_i't] \quad (4)$$

Thus graphs of experimentally determined values of $\ln(b_i/b_i^0)$ versus time or versus $\ln(b_1/b_1^0)$ should yield straight line for systems which exhibit first-order behavior and negligible isotope effect.

The selectivity M of the reaction can be characterized by the average number of deuterium atoms in the initial product:

$$M = \text{initial}\left[\sum_{i=1}^{n} ia_i \bigg/ \sum_{i=1}^{n} a_i\right] = \frac{n\lambda_i'}{\lambda_n'} \quad (5)$$

which for neopentane, studied in terms of t-butyl fragments, is

$$M = \frac{9\lambda_1'}{\lambda_9'} = \frac{12 + 9\beta}{12 + \beta} \quad (6)$$

For values of β near zero, the product distribution has binomial character and M approaches 1. For non-zero values of β, especially $\beta > 0.3$, the product distribution deviates significantly from binomial character. For very large β values, M approaches n.

III. EQUIPMENT AND OPERATING PROCEDURES

A. Catalyst Preparation

Platinum catalysts were prepared by impregnation of γ-alumina supports (Rhone-Poulenc, Inc., GOD-30) with chloroplatinic acid solution. The alumina beads were of spherical geometry and had the following properties: diameter, 0.38 cm; bulk density, 0.3 g/ml; surface area, 150 m^2/g; total pore volume, 1.70 ml/g; and average pore diameter, 450 Å.

The beads were dried at 393 K for 2 h and then impregnated 48 h with an aqueous solution containing the desired H$_2$PtCl$_6$ con-

tent. Upon removal from the impregnating solution by filtering, the beads were sparingly surface washed with deionized water and surface dried. After catalysts were dried at 393 K for 2 h, they were reduced in flowing hydrogen for 4 h at 723 K in a tube furnace. Sample 6 was reduced at 773 K for 6 h.

The platinum content of the catalysts was determined by spectrophotometric analysis of the impregnating solutions using a Bausch & Lomb spectrophotometer. All catalysts were crushed to 200 mesh prior to characterization.

B. Catalyst Characterization

1. Hydrogen chemisorption. One of the three methods employed to determine average crystallite size of the catalysts was hydrogen chemisorption in a static system. The system was equipped with an Edwards' Cryo-cooled Diffstak-63 oil diffusion pump, an EDM2 mechanical vacuum pump, and two MKS Baratron 200A pressure gauges with ranges from 0 to 100 and 0 to 1000 Torr. The adsorption cell, also used as the reactor in kinetic studies, was made of quartz. It was connected to the system with Cajon Ultra-Torr fittings.

Prior to chemisorption measurements, the catalyst samples were evacuated at 723 K for 16 h in a Thermolyne tube furnace. The chemisorption data were taken at room temperature using hydrogen gas (Matheson Ultra High Purity Hydrogen, 99.999%) which was passed through a Deoxo hydrogen purifier and a liquid nitrogen trap.

2. X-ray line broadening. The catalyst samples (200 mesh) were mounted on a rotating specimen holder of a General Electric XRD-6 diffractometer equipped with a Warren double-bent LiF monochromator and automated in scanning. A copper target tube operating at 35 kV and 17 mA was used in conjunction with a proportional counter. The diffracted intensity of (311) platinum reflection was step-scanned from 76 to 86 degrees of 0.1-degree intervals re-

cording the time required for the accumulation of 3000 counts at each point.

The true intensity of the (311) reflection was obtained after subtraction of background caused by the γ-alumina carrier. The instrumental broadening was determined by using magnesium oxide which was sintered at 1273 K for 16 h and therefore effectively infinite in crystallite size with respect to the platinum samples. The observed diffraction profile was corrected for instrumental broadening using Warren's correction (*11*).

3. Electron microscopy. The samples were analyzed using the following procedure. Approximately 1 mm^3 of powdered sample was mixed with methylmethacrylate which was then polymerized overnight at 321 K (2% benzoyl peroxide as curing agent). Sections from the resin block were cut in a Reiche OM-U2 ultramicrotome using a diamond knife and then mounted on carbon-coated TEM grids. Electron micrographs were made on a Phillips EM-200 electron microscope at 200 kV.

Carl-Zeiss Particle Size Analyzer TGZ 3 was used in determining the size distributions. An average of 800 particles was counted for each sample. The measuring range of the instrument consists of 48 continuous categories permitting measurement of particles of 0.5 to 9.2 mm in diameter from the electron micrographs.

B. Reaction Studies

Kinetic data were obtained in a glass (Pyrex and quartz) recirculation system (total volume 850 cm^3) which consisted of a doubly acting magnetic pump, mixing bulb, quartz U-tube reactor, sampling loop, and circulation tubing. Circulating gas flow rate was 2000 cm^3/min measured by a rotameter temporarily connected to the system. The reactor was a 1.27 mm o.d. quartz U-tube in which a catalyst bed was packed between plugs of quartz wool. A thermo well was positioned at the center of the catalyst bed. A Leeds-Northrup zero voltage power pack supplied power to the tube furnace which

was placed around the U-tube reactor. Temperature was controlled by a Leeds-Northrup Electromax III proportional controller. The catalysts were pretreated between experiments by evacuating (10^{-7} Torr) overnight at 723 K. Before each run, the reactor was charged with neopentane (Matheson CP grade, 99.87%) and deuterium that had been passed through a liquid nitrogen trap. Gas mixture pressure was 65 Torr. Neopentane–deuterium ratio was typically 1 : 450. The reactants were mixed by the recirculation pump, bypassing the catalyst bed. The run was started by directing the gas flow through the catalyst bed. The sample loop consisted of a 1.46-cm³ volume connected via stopcocks to the reactor, to vacuum, and to a mass spectrometer (Kratos MS10S). Sampling did not significantly change the reactor pressure since the sampling volume was less than 0.20% of total reactor volume. The mass spectrometer was operated at 15 eV in order to minimize fragmentation. The parent ion of neopentane is of low intensity in the mass spectrometer; therefore, reaction products were analyzed in terms of t-butyl fragments (10). Scans of the mass range 57 through 66 (C_4H_9 through C_4D_9) were recorded after background scans were taken. Raw data were corrected for fragmentation and natural abundances of C^{13} and deuterium. The analysis of data and model simulation were carried out using a CDC Cyber 74 computer.

IV. RESULTS AND DISCUSSION

A. Catalyst Characterization

It has been observed in previous studies that sintering, when used as a method to vary crystallite size, may lead to apparent-crystallite size effects (14). Heat treatments in air to produce catalysts with different mean crystallite sizes will increase the range of sizes in a given catalyst giving rise to a broad size distribution (5). In this study, however, crystallite size variation was effected by changing the metal content

of the catalysts (i.e., 0.28 to 2.68% Pt). This method of controlling crystallite size was found to be very sensitive to catalyst preparation conditions. Since the reproducibility of preparing catalysts which had identical crystallite sizes was poor, it was necessary to make a large number of catalysts, characterize them, and select from them those in the desired range of crystallite size for further study. Tables 1 and 2 show, respectively, the results of hydrogen chemisorption and a comparison of metal crystallite size as calculated from hydrogen chemisorption, X-ray line broadening, and TEM. Agreement is very good for five of the six catalysts; however, only one technique—hydrogen chemisorption—could be used on the catalyst with the smallest crystallite size. This catalyst had a calculated crystallite diameter of 8 Å. Hydrogen chemisorption data were converted to platinum surface area by assuming an adsorption stoichiometry of 1 : 1 between the hydrogen and the surface platinum atom (4, 15, 19). In converting hydrogen chemisorption measurements to specific surface areas, it was assumed that a platinum surface atom occupies an area of 8.9 Å² on the catalyst surface. Average crystallite sizes were calculated from the metal surface areas by assuming the platinum crystallites to be cubes with five exposed faces. In obtaining the isotherms, approximately 30 min were allowed for equilibrium to be established. The hydrogen uptake corresponding to a

TABLE 1

Hydrogen Chemisorption Results

Catalyst	H₂ uptake (μmol/g)	Pt dispersion (H atoms / Pt atoms total)
1	7.47	1.06
2	23.29	0.45
3	9.47	0.19
4	7.56	0.13
5	7.22	0.11
6	3.23	0.05

TABLE 2

Comparison of Pt Crystallite Size (Å) Determined by Three Different Techniques; Size Distribution

Catalyst	TEM			H_2 Chemis. D_S	XRL D_V	Crystallite size distribution by TEM	
	D_N	D_S	D_V			Standard deviation (Å)	Spread about the mean (%)
1	—	—	—	8	—	—	—
2	22	23	26	19	—	5.4	24.3
3	50	53	57	46	56	10.4	20.8
4	66	70	75	64	69	35.6	53.9
5	75	78	82	76	84	26.3	35.1
6	168	172	177	178	160	27.6	16.8

Note. D_N, D_S, D_V—respectively: numerical, surface, and volume average crystallite size.

monolayer coverage was obtained from the intercept of the isotherm at zero pressure. A blank was run on the support and the adsorption of hydrogen on the support at room temperature was found to be negligible.

Hydrogen pressures up to 30 Torr were used in determining the isotherms. Use of higher pressures (up to 90 Torr) resulted in hydrogen uptakes very close to those obtained at low pressures. For sample 2, the high-pressure and low-pressure uptakes were 21.53 and 23.29 μmol H_2/g catalyst, respectively.

The volume-average Pt crystallite sizes were determined from X-ray line broadening data using Scherrer's formula:

$$d = K\lambda/\beta' \cos \theta$$

where

K = shape factor = 0.94
λ = X-ray wavelength
θ = Bragg angle
β' = linebreadth after correction for instrumental broadening.

The experimentally observed broadening was corrected for instrumental effects using Warren's correction:

$$\beta' = (B^2 - b^2)^{1/2}$$

where b = line breadth caused by instru-

mental broadening and B = line breadth of the sample observed under experimental conditions. Figure 1 is a diffraction profile for one catalyst sample. Linebreadths were determined as widths at half-maximum intensity on such profiles. No peaks were observed for Samples 1 and 2; therefore their analyses by X-ray line broadening were not possible.

The crystallite size distributions for the catalysts were determined by electron microscopy. Six electron micrographs were made for each catalyst. The magnification was 300,000× for all the micrographs except for those of Sample 6 which were photographed at 192,000×. The size distributions of one of the samples is shown in Fig. 2. Sufficiently accurate measurements were not possible at very small diameters such as those in Sample 1. The number-average, surface-average, and volume-average diameters determined from the size distributions are given in Table 2. These calculations were made as follows:

$$D_N = \Sigma n_i d_i / \Sigma n_i$$

$$D_s = \Sigma n_i d_i^3 / \Sigma n_i d_i^2$$

$$D_v = \Sigma n_i d_i^4 / \Sigma n_i d_i^3$$

where

di = diameter of crystallite (Å)
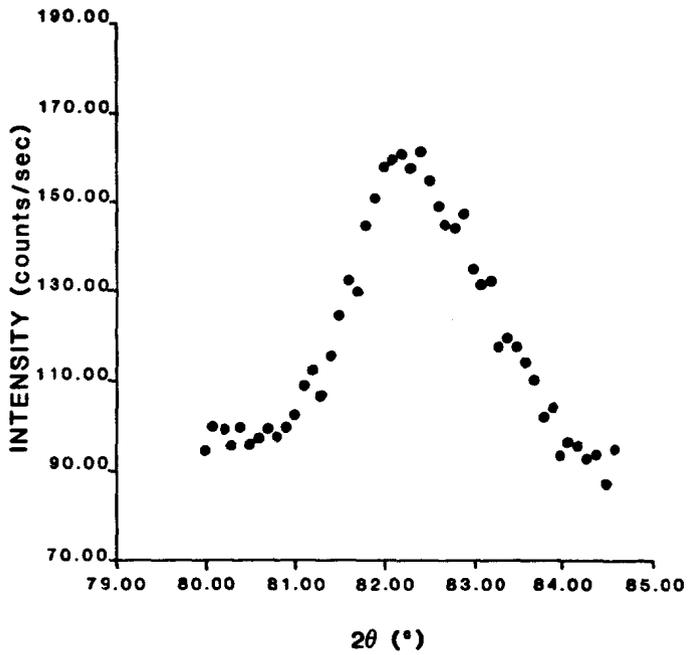n_i = number of crystallites of diameter d_i

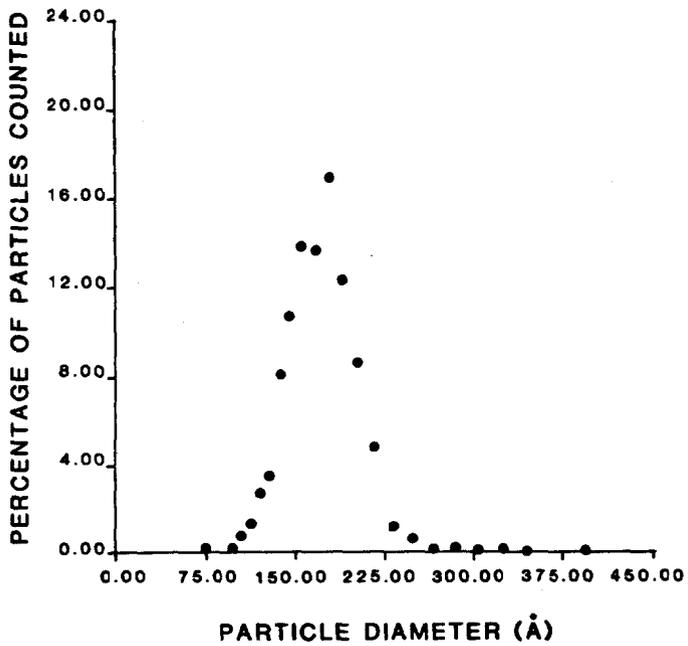FIG. 1. X-Ray line broadening pattern for Sample 5.

FIG. 2. Crystallite size distribution for Sample 6.

According to Luss (12), the average crystallite size is a single statistic of the size distribution and many different distributions have the same average. Hence, if a reaction is demanding and the activity is not a linear function of average crystallite size, two distributions with the same average may have different catalytic behavior. Thus, to fully describe the distribution, the standard deviation and the spread about the mean crystallite size, defined as the ratio of standard deviation to the mean, have to be determined along with average size. The results of such calculations are shown in Table 2. Samples 4 and 5 have relatively broad size distributions: the values for spread about the mean size for these two catalysts are higher than those for the other catalysts.

B. Neopentane–Deuterium Exchange Reaction

Preliminary runs on test catalysts were conducted to establish pretreatment conditions which would lead to reproducible experimental results. Evacuating the catalyst at 10^{-7} Torr and 473 K for 2 h between reaction experiments led to a decline in activity from one run to the next. Relative activities for three such runs at 393 K from first to last were 1 : 0.45 : 0.27. Overnight bake-out at 723 K at 10^{-7} Torr yielded reproducible results for three successive runs. Relative activities for these runs from first to last were 1 : 0.90 : 0.94.

No deactivation was observed during a reaction run as evidenced by the linearity of semilog plots of characteristic species concentration versus time (see Fig. 3, for example).

A total of 62 reaction runs were conducted. Table 3 shows results for one of the catalysts. On the average, runs were continued until about a 60% neopentane conversion was achieved. In order to test the reproducibility of results from batch to batch, experiments were run on two different batches of each of the six catalysts. The support was found to possess negligible activity for neopentane exchange in an experiment at 673 K. Three runs were conducted at different circulating gas rates (2000,
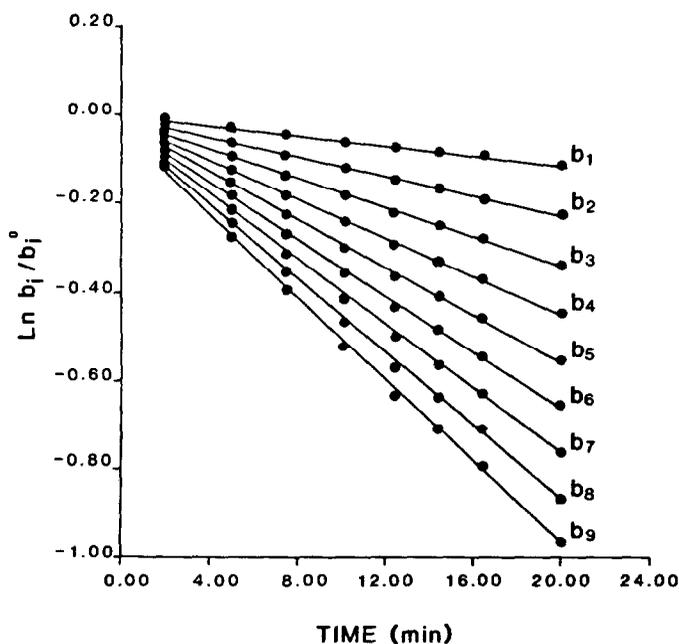
FIG. 3. Decay of characteristic species with time for Run 1-1-1.

TABLE 3

Kinetic Parameters for Neopentane–Deuterium Exchange Reaction for Catalyst No. 3

Cat.-Batch-Run	T (°K)	$k\ddagger$ $\left(\dfrac{cm^3 \text{ gas}}{s \cdot cm^3 \text{ cat.}}\right)$	k $\left(\dfrac{cm^3 \text{ gas}}{s \cdot mg \text{ Pt}_s}\right)$	β	M_β	$\psi \times 10^3$
3-1-5	353	0.30	0.15	0.13	1.08	1.7
3-1-4	365	0.54	0.28	0.18	1.12	3.1
3-1-2	383	1.57	0.82	0.41	1.27	2.0
3-1-1	402	3.00	1.55	0.70	1.44	3.0
3-1-3	416	8.00	4.13	1.32	1.79	5.3
3-2-7	304	0.01	0.005	0.01	1.01	2.0
3-2-6	304	0.01	0.006	0.02	1.01	1.3
3-2-5	305	0.01	0.006	0.02	1.01	1.8
3-2-10	341	0.06	0.03	0.12	1.08	1.4
3-2-9	342	0.06	0.03	0.08	1.05	1.6
3-2-8	343	0.08	0.04	0.13	1.09	2.1
3-2-3	359	0.38	0.20	0.25	1.16	9.0
3-2-2	359	0.45	0.23	0.26	1.17	7.0
3-2-1	360	0.40	0.21	0.22	1.14	6.0
3-2-4	360	0.40	0.21	0.23	1.15	7.0

1000, 600 cm^3/min) under identical conditions. The activity and selectivity for these runs were equal within experimental accuracy.

Since experiments were run on crushed catalysts, it was initially assumed that the mass transfer effects were negligible. The validity of this assumption was checked by a two-parameter model which included the intraparticle diffusion effect (6). Effectiveness factor values were very close to 1 for each experiment.

Data for all of the runs were found to obey first-order kinetic behavior with negligible isotope effect in accordance with Eq. (4). Figures 3 and 4, for example, show the linear behavior for $\ln(b_i/b_i^0)$ versus time and $\ln(b_i/b_i^0)$ versus $\ln(b_1/b_1^0)$ for typical runs. The symbols on these graphs are experimental values while the straight lines are those determined by linear regression analysis. The slopes of the $\ln(b_i/b_i^0)$ vs $\ln(b_1/b_1^0)$ graph—λ_i'/λ_1—can be used as a measure of selectivity of the reaction. For systems which exhibit binomial distributions of products, $\lambda_i'/\lambda_1' = i$. Deviation from bino-

mial character is indicated by deviation of λ_i'/λ_1' from i.

In an attempt to correlate all of the reaction data and describe deviation of product distribution from binomial, reactor data were compared with predictions of Dwyer's model of single-step surface exchange influenced by desorption, β, effects (Eqs. (1) and (3)). For each run, the value of β was adjusted until a minimum value of an objective function Ψ (standard deviation) was found

$$\Psi = \left\{ \sum_{j=1}^{T} \sum_{i=1}^{n} [a_{i,\exp} - a_{i,\text{calc}}]_j^2 / n \cdot T \right\}^{1/2}$$

where T is the number of samples taken during the run. The values of $a_{i,\exp}$ and $a_{i,\text{calc}}$ for each sample were determined at the same neopentane conversion. Table 3 contains parameter values as well as selectivity values, M, for runs on Catalyst No. 3. The range of Ψ values for the 62 runs is from 0.0006 to 0.028; however, for runs conducted at temperatures below 400 K, the range was from 0.0006 to 0.009. This range
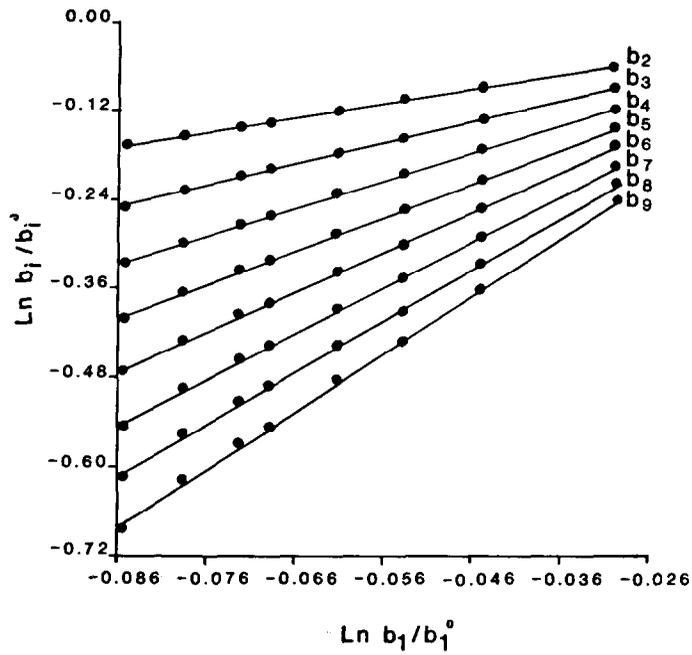
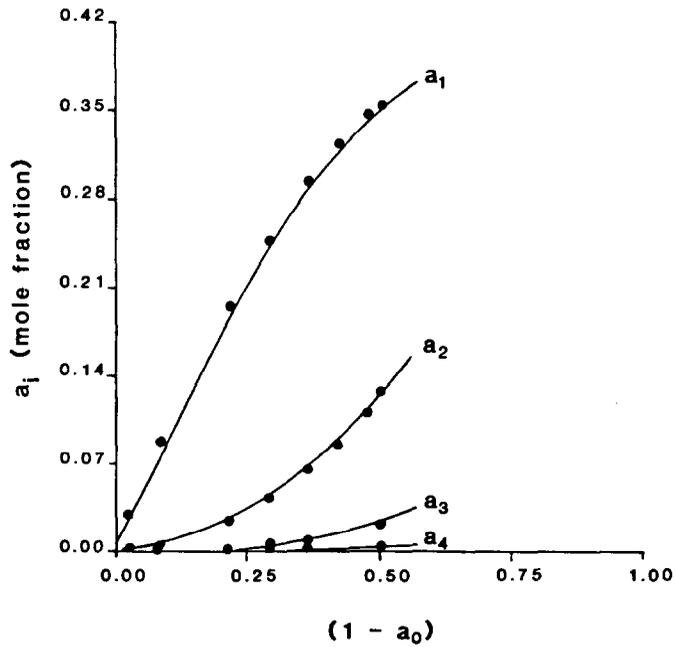FIG. 4. Relative change of characteristic species for Run 1-1-2.

FIG. 5. Experimental and calculated real species concentrations versus neopentane conversion for Run 1-1-2.

represents a deviation of less than 0.06 to 0.9% of the total neopentane isomer content. Figure 5 shows graphically the agreement between experimental and calculated a_i values for one run.

The β values are approximately proportional to specific activity, k, at lower values of k, for each of the catalysts. As k approaches zero, β also approaches zero. This β versus k behavior is in agreement with neopentane–deuterium exchange on supported Pd (6, 9) and is in support of an exchange mechanism in which neopentane initially adsorbs on the catalyst as an undissociated molecule. The β parameter can be interpreted as the relative rate of exchange of the adsorbed molecule to that of desorption.

Figure 6 shows the β versus k (in units of cm^3 gas/s · cm^3 cat.) relationship for low k values where the relationship is approximately linear. Figure 7 shows the selectivity (M_β) versus k relationship for all of the data. The graphs are identical in format to those previously presented by Dwyer et al.

(7) and contain data from the three previous studies on supported Pd (6, 7, 9). Figure 6 shows a much smaller influence of k on β for the Pt catalysts versus the Pd catalysts. The slopes of straight lines through these data are 31, 8.4, and 2.6 for the Pd data and 0.14 for the Pt data. The β versus k trend for the Pt catalyst coincides approximately with data for Pd which had been oxygen treated—a method which Dwyer et al. used to lower β in catalyst beads containing supported Pd. The reason that data for the three studies on Pd lie on different lines is not understood. Figure 7 shows that even at high activity levels the selectivity is much less dependent upon k for Pt catalysts than for Pd catalysts.

In order to examine the effect of metal dispersion on catalyst performance, kinetic data for each of the Pt catalysts were examined separately. Activation energies were determined by Arrhenius plots of specific activity. Good straight lines were obtained for each of the catalysts (see Fig. 8 for example). The activation energies (Table 4)
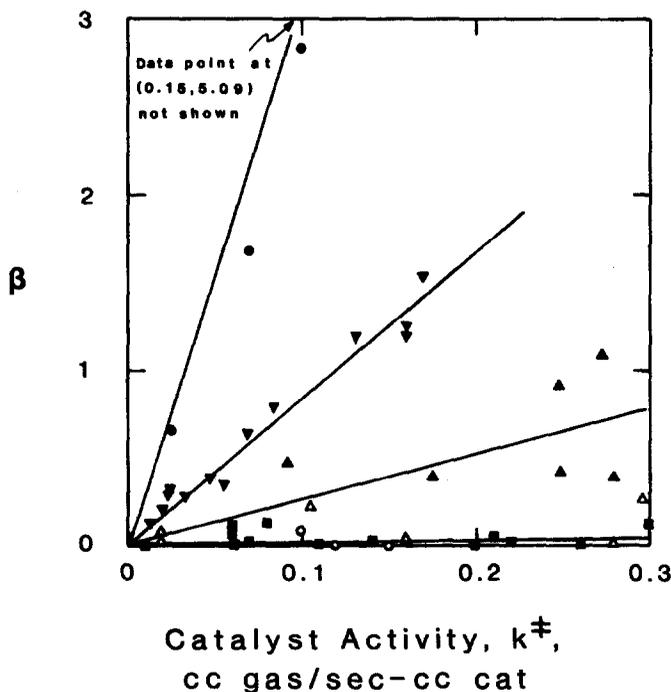

FIG. 6. Desorption parameter versus activity (see Fig. 7 for key to symbols).
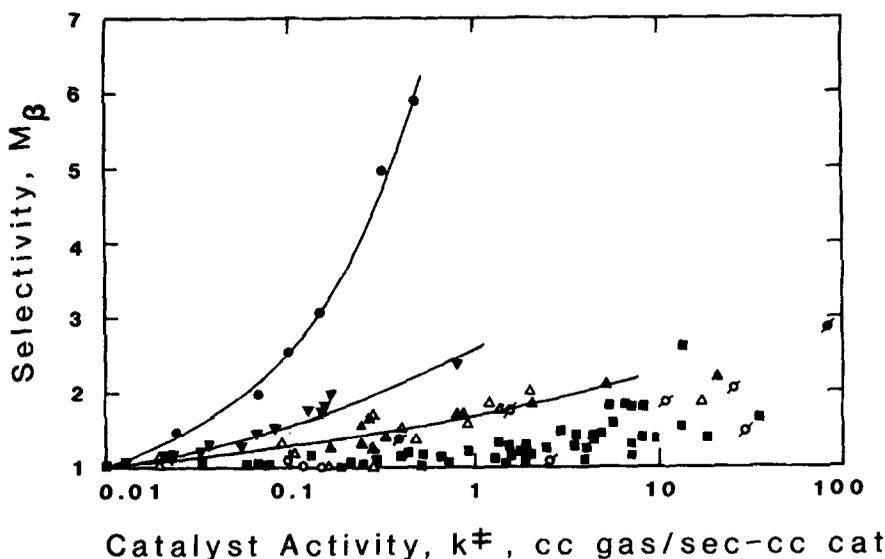
Fig. 7. Selectivity versus activity. Sources of data: ■, this work; ▼, Ref. (6); ●, Ref. (7) ($\frac{1}{8}$-in. beads); ◢, Ref. (7) (<100 mesh particles); ▲, Ref. (9). Solid symbols: no O_2 pretreatment. Open symbols: with O_2 pretreatment.

fall approximately in the same range. The average value is 12.9 ± 0.5 kcal/mol where the uncertainty term represents the average of the absolute value of the deviations from the mean. This represents approximately a 4% deviation.

Values of k (in units of cm³ gas/s · mg of surface Pt) for each catalyst were compared at two different temperature levels (see Table 5). These k values were obtained from straight lines fitted through the experimental data on Arrhenius graphs. Similarly, it

was found that graphs of ln β versus $1/T$ could be accurately fitted with straight lines. The β values in Table 5 were taken from these graphs.

The average values of k in Table 5 are 0.22 and 1.92 at 353 and 398 K, respectively. Although there is some deviation of individual values about the mean (about 27% at both temperatures), there is no obvious trend in the data that would indicate significant structure sensitivity. In contrast to these results, a typical example of a

TABLE 4

Activation Energy versus Pt Dispersion

Catalyst	D_s (Å)	E_{ACT} (kcal/g mol)
1	8	12.3
2	19	13.2
3	46	14.0
4	64	12.8
5	76	13.1
6	178	12.1
Average		12.9

TABLE 5

Influence of Pt Crystallite Size on Activity and Selectivity

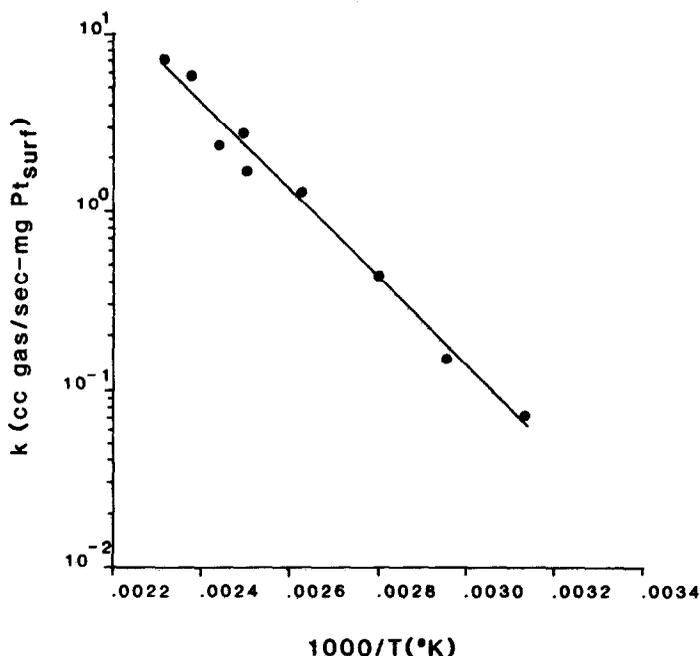| D_s (Å)	$k \left(\frac{cm^3 \, gas}{s \cdot mg \, Pt_s} \right)$		β		Selectivity, M	
	353 K	398 K	353 K	398 K	353 K	398 K
8	0.28	2.08	0.05	0.27	1.03	1.17
19	0.24	2.30	0.05	0.43	1.04	1.28
46	0.13	1.34	0.15	0.84	1.10	1.52
64	0.24	2.19	0.09	0.46	1.06	1.29
76	0.32	2.63	0.05	0.44	1.04	1.28
178	0.13	0.95	0.03	0.18	1.02	1.12
Average	0.22	1.92				

FIG. 8. Arrhenius plot for Sample 1.

structure sensitive reaction reported in the literature—the hydrogenolysis of neopentane on supported Pt (which is encountered at temperatures greater than those of the present study)—exhibited greater than 300-fold variation in specific activity with Pt dispersion (*1*).

The β parameter, upon which selectivity of the reaction depends, exhibits a weak trend with metal dispersion. At both temperatures, a maximum β occurs at mean Pt crystallite size between 19 and 64 Å. This range corresponds to a Pt dispersion of 0.45 to 0.13 H atoms/Pt atoms total. The selectivity, M, calculated from β values is also shown in Table 5. In view of the suspected mechanism of the reaction previously discussed and the observed insensitivity of specific activity to metal dispersion, the change in β is possibly due to a change in the rate of desorption of molecularly adsorbed neopentane.

Van Hardeveld and Hartog (*17*) have shown that there is greater activity for exchange and deuteration and selectivity for multiple exchange for benzene–deuterium exchange on iridium catalysts with average crystallite sizes of 37 Å than on 8 or 600 Å. They attributed this maximum to the predominance of edge sites at intermediate crystallite sizes.

The possibility therefore exists that edge sites contributed to the sensitivity of the β parameter hence the selectivity for the neopentane–deuterium exchange reaction in this study. The decrease in selectivity below a certain crystallite size is for some systems indicative of the fact that a minimum crystallite size is required. Coenan *et al.* (*2*) observed a decrease in activity below 12 Å for benzene hydrogenation on nickel catalysts. Den Otter and Dautzenberg (*3*) have observed that upon treatment in hydrogen at high temperatures (>773 K), Pt/Al₂O₃ catalysts with highly dispersed particles form an alloy with aluminum from the support; however, in the present case, such an effect is unlikely because the catalysts were never subjected to such high temperatures. Metal support interaction

and distribution of particle sizes make a complete explanation of the selectivity data impossible.

CONCLUSIONS

It has been shown that in the absence of mass transport limitations the neopentane–deuterium exchange reaction over supported Pt on γ-Al$_2$O$_3$ catalysts can be accurately represented by a model previously developed to explain this reaction over supported Pd. The model is based upon first-order behavior in neopentane and negligible isotope effect. Deviation of product distribution from "binomial" character can be accurately described in terms of the desorption parameter β. However, the β dependence on specific activity is much less severe for Pt catalysts than for Pd catalysts. This feature makes Pt a better choice of catalysts to use with the neopentane-deuterium exchange for studying mass transport effects.

The catalyst activity has been shown to be facile over the total range of Pt crystallite sizes studied; the selectivity is only mildly sensitive to Pt crystallite size and exhibits a weak maximum within the size range 19 to 64 Å. The reaction might therefore be a suitable probe for studying the combined effects of mass transport limitation and distribution of active ingredient in nonuniformly active catalysts.

ACKNOWLEDGMENTS

REFERENCES

1. Boudart, M., Aldag, A. W., Ptak, L. D., and Benson, J. E., *J. Catal.* **11,** 35 (1968).
2. Coenen, J. W. E., van Meerten, R. Z. C., and Rijnten, T., "Proceedings, 5th International Congress on Catalysis" Paper 45, p. 671. 1973.
3. den Otter, G. J., and Dautzenberg, F. M., *J. Catal.* **53,** 116 (1978).
4. Dorling, T. A., Burlace, C. J., and Moss, R. L., *J. Catal.* **12,** 207 (1966).
5. Dorling, T. A., and Moss, R. L., *J. Catal.* **5,** 111 (1965).
6. Dwyer, F. G., Eagleton, L. C., Wei, J., and Zahner, J. C., *Proc. Roy. Soc. A* **302,** 253 (1968).
7. Dwyer, F. G., Lago, R. M., Wei, J., and Zahner, J. C., "Proceedings, IVth International Congress on Catalysis, Moscow," 1968.
8. Ernst, W. R., and Daugherty, D. J., *AIChE J.* **24**(5), 935 (1978).
9. Ernst, W. R., and Wei, J., *J. Catal.* **39,** 303 (1975).
10. Kemball, C., *Trans. Faraday Soc.* **50,** 1344 (1954).
11. Klug, H. P., and Alexander, L. E., "X-Ray Diffraction Procedures for Polycrystalline and Amorphous Materials." Wiley, New York, 1974.
12. Luss, D., *J. Catal.* **23,** 119 (1971).
13. Mikovsky, R. J., and Wei, J., *Chem. Eng. Sci.* **18,** 253 (1963).
14. Sagert, N. H., and Pouteau, R. M. L., *Can. J. Chem.* **51,** 3588 (1973).
15. Spenadel, L., and Boudart, M., *J. Phys. Chem.* **64,** 204 (1960).
16. Shyr, Y. S., and Ernst, W. R., *J. Catal.* **63,** 425 (1980).
17. van Hardeveld, R., and Hartog, F., *in* "Advances in Catalysis" (D. D. Eley, H. Pines, and P. B. Weisz, Eds.), Vol. 22, p. 75. Academic Press, New York, 1972.
18. Wei, J., and Prater, C. D., *in* "Advances in Catalysis" (D. D. Eley, P. W. Selwood, and P. B. Weisz, Eds.), Vol. 13, p. 203. Academic Press, New York, 1962.
19. Wilson, G. R., and Hall, W. K., *J. Catal.* **17,** 190 (1970).
20. Yurchak, S., Mobil Research and Development Corporation, Paulsboro, New Jersey, private communication with W. Ernst.
21. Zahner, J. C., "Proceedings, 1st International Symposium Chemical Reaction Engineering," Washington, D.C., 1970.